

# Evaluation of electrical parameters of electron and proton irradiated GaInP/GaAs/InGaAs metamorphic solar cells

© Z.X. Wang<sup>1</sup>, M.Q. Liu<sup>2</sup>, T.B. Wang<sup>1</sup>, M. Li<sup>1</sup>, G.H. Tang<sup>1</sup>, A. Aierken<sup>1,¶</sup>, L. Zhong<sup>2</sup>

<sup>1</sup> School of Energy and Environment Science, Yunnan Normal University, Kunming, 650500, China

<sup>2</sup> Institute of Electronic Engineering, China Academy of Engineering Physics, Mianyang, 621900, China

¶ E-mail: erkin@ynnu.edu.cn, zhongle\_mtrc@caep.cn

Received April 26, 2023

Revised September 27, 2023

Accepted for publication April 3, 2024

Changes of electrical parameters in electron and proton irradiated metamorphic GaInP/GaAs/InGaAs solar cells have been investigated experimentally and numerically simulation by single diode mode. Basic electrical parameters of solar cells under 1 MeV electron and 10 MeV proton irradiation with different displacement damage doses were extracted. The results show that the dark current, ideal factor and series resistance of solar cells increase and parallel resistance decrease with the increase of the irradiation fluence. A simple method for evaluating radiation effects of the electrical parameters of solar cells is established.

**Keywords:** GaAs solar cell, electron and proton irradiation, curve fitting, displacement damage dose.

DOI: 10.61011/SC.2024.02.58364.4919

## 1. Introduction

Solar cells have been widely used various applications, and, evaluating cell performance in harsh environment, such as in space application, became an important tool to optimize solar cell structure and design future radiation hardened and high efficiency solar cells [1,2]. Currently, both single and the double-diode models are frequently used for extracting solar cell electrical parameters, including photogenerated current  $I_{ph}$ , dark current  $I_0$ , parallel resistance  $R_{sh}$ , series resistance  $R_s$ , and ideal factor  $n$  [3]. The solar cell electrical parameters can be investigated by numerical calculation and experimental data fitting [4,5].

Shubham Raj et al. used linear slope equation and Newton–Raphson technique to obtain  $R_s$ ,  $R_{sh}$ ,  $I_0$  and  $n$  of a silicon solar cell [6]. Lim et al. extracted diode parameters from a  $I-V$  curve by using linear differential equation and single diode model [7]. Bouzidi et al. extracted  $I_s$  (saturation current),  $R_s$ ,  $n$ , and  $G_{sh}$  (shunt conductance) of polycrystalline silicon solar cell from a dark DIV (dark current-voltage) curve by using single diode model [8]. Haouari–Merbah et al. proposed an approach for extracting solar cell electrical parameters by least square fitting in the near short-circuit and near open-circuit voltage region of a  $I-V$  curve [9].

A method with great reliability and accuracy was proposed by Buhler et al. that able to post-process  $I-V$  curves to extract the electrical parameters of photovoltaic devices [10]. Sabadus et al. extracted and solved the four-parameter model in the single-diode model by combining the Taylor's series using current equation with the  $I-V$  curve of STC photovoltaic modules [11].

In addition, there are other solutions for extracting electrical parameters of solar cells through simulated anneal-

ing algorithm [12], semi-analytic modified Hooke–Jeeves method [4], non-iterative technique [13], Shockley's equation [14], Lambert W function [15], and other methods. Furthermore, Ben Or et al. studied the electrical parameters of GaInP/GaAs/Ge triple-junction solar cells using a single diode model, and proposed a mathematical method to extract conventional parameters, breakdown voltage and additional parameters from the measured  $I-V$  characteristics [16]. There are, however, only few research studies that combining the  $I-V$  curve fitting method with the radiation damage mechanism to predict the electrical parameters of solar cells [17].

In this paper, we studied we studied and numerically fitted the  $I-V$  curves of triple-junction GaInP/GaAs/InGaAs (inverted metamorphic, IMM) and GaInP/GaAs/Ge (lattice-matched, LM) solar cells under 10 MeV proton and 1 MeV electron radiation at various displacement damage doses (DDD). The correlations between the changes of solar cell electrical parameters and its radiation hardness have been discussed.

## 2. Materials and methods

Figure 1, *a* and *b* show the IMM  $Ga_{0.5}In_{0.5}P/GaAs/In_{0.3}Ga_{0.7}As$  solar cell and LM  $Ga_{0.5}In_{0.5}P/In_{0.03}Ga_{0.97}As/Ge$  solar cell structures, respectively. Solar cells are fabricated by a MOCVD system and each device is prepared in  $3 \times 4 \text{ cm}^2$  size. The detailed epitaxial growth and cell fabrication processes have been reported in detail in the Ref. [18].

The irradiation experimentations were carried out by using a high frequency and high voltage electron accelerator and a tandem electrostatic proton accelerator. Table 1 listed

a			b		
$p\text{-In}_{0.3}\text{GaAs}$	Cap	(500 nm)	$n\text{-GaAs}$	Cap	(500 nm)
$p\text{-In}_{0.3}\text{AlGaAs}$	BSF	(100 nm)	$n\text{-Ga}_{0.5}\text{InP}$	Window	(100 nm)
$p\text{-In}_{0.3}\text{GaAs}$	Base	(2000 nm)	$n\text{-Ga}_{0.5}\text{InP}$	Emitter	(100 nm)
$n\text{-In}_{0.3}\text{AlGaAs}$	Emitter	(200 nm)	$p\text{-Ga}_{0.5}\text{InP}$	Base	(700 nm)
$n\text{-In}_{0.3}\text{GaAs}$	Window	(200 nm)	$p\text{-Ga}_{0.5}\text{InP}$	BSF	(100 nm)
$n\text{-AlGaInAs}$ Step-Grade (4000 nm)			Tunnel junction		
Tunnel junction			$n\text{-Al}_{0.5}\text{InP}$	Window	(100 nm)
$p\text{-AlGaAs}$	BSF	(100 nm)	$n\text{-In}_{0.03}\text{GaAs}$	Emitter	(100 nm)
$p\text{-GaAs}$	Base	(3000 nm)	$p\text{-In}_{0.03}\text{GaAs}$	Base	(2000 nm)
$n\text{-GaAs}$	Emitter	(1000 nm)	$p\text{-Al}_{0.35}\text{GaAs}$	BSF	(100 nm)
$n\text{-AlInP}$	Window	(100 nm)	DBR (2500 nm) GaAs/Al <sub>0.3</sub> GaAs		
Tunnel junction			Tunnel junction		
$p\text{-AlGaAs}$	BSF	(100 nm)	$n\text{-GaAs}$	Buffer	(600 nm)
$p\text{-GaAs}$	Base	(700 nm)	$n\text{-Ga}_{0.5}\text{InP}$	Window	(300 nm)
$n\text{-GaAs}$	Emitter	(100 nm)	$n\text{-Ge}$		
$n\text{-AlInP}$	Window	(100 nm)	$p\text{-Ge}$	Substrate	(175)
$n\text{-InGaAs}$	Cap	(500 nm)			
AllInP Etch-stop					
$n\text{-GaAs}$ Substrate					

**Figure 1.** (a) IMM Ga<sub>0.5</sub>In<sub>0.5</sub>P/GaAs/In<sub>0.3</sub>Ga<sub>0.7</sub>As triple-junction solar cell and (b) LM Ga<sub>0.5</sub>In<sub>0.5</sub>P/In<sub>0.03</sub>Ga<sub>0.97</sub>As/Ge triple-junction solar cell structures.

**Table 1.** Irradiation fluence of electron and proton radiation

10 MeV proton (p/cm <sup>-2</sup> )	DDD (MeV/g)	1 MeV electron (e/cm <sup>-2</sup> )
0	0	0
$2.18 \cdot 10^{12}$	$1.58 \cdot 10^{10}$	$5 \cdot 10^{14}$
$4.35 \cdot 10^{12}$	$3.16 \cdot 10^{10}$	$1 \cdot 10^{15}$

the selected irradiation fluence of electron and proton beams and corresponding displacement damage dose (DDD) is calculated by Eq. (1):

$$\text{DDD} = \phi \times \text{NIEL}, \quad (1)$$

where DDD (MeV/g) is displacement damage dose,  $\phi$  (e,p/cm<sup>-2</sup>) is the irradiation fluence, and NIEL (MeV cm<sup>2</sup>/g) is the non-ionizing energy loss for corresponding materials. An OAI TSS-156 solar simulator was used to characterize  $I$ - $V$  characteristics of solar cells, and the

measurement was conducted at 25°C under AM0 spectrum (136.7 mW/cm<sup>2</sup>).

The single diode current model, showed in Eq. (2) [3,7,19], used to fit solar cell  $I$ - $V$  curves, and  $I_{\text{ph}}$ ,  $I_0$ ,  $n$ ,  $R_{\text{sh}}$  and  $R_s$  of the solar cells have been extracted from the experimental data

$$I = I_{\text{ph}} - I_0 \left[ \exp\left(\frac{V + IR_s}{nk_0T}\right) - 1 \right] - \frac{V + IR_s}{R_{\text{sh}}}. \quad (2)$$

### 3. Results and discussions

#### 3.1. Fitting results of IMM triple-junction solar cells

The measured and simulated  $I$ - $V$  curves of electron and proton irradiated IMM GaInP/GaAs/InGaAs solar cells with different irradiation doses are shown in Figure 2, *a* and *b*. The experimental data shows that  $V_{oc}$  (open circuit voltage) and  $FF$  (filling factor) decreased significantly with the

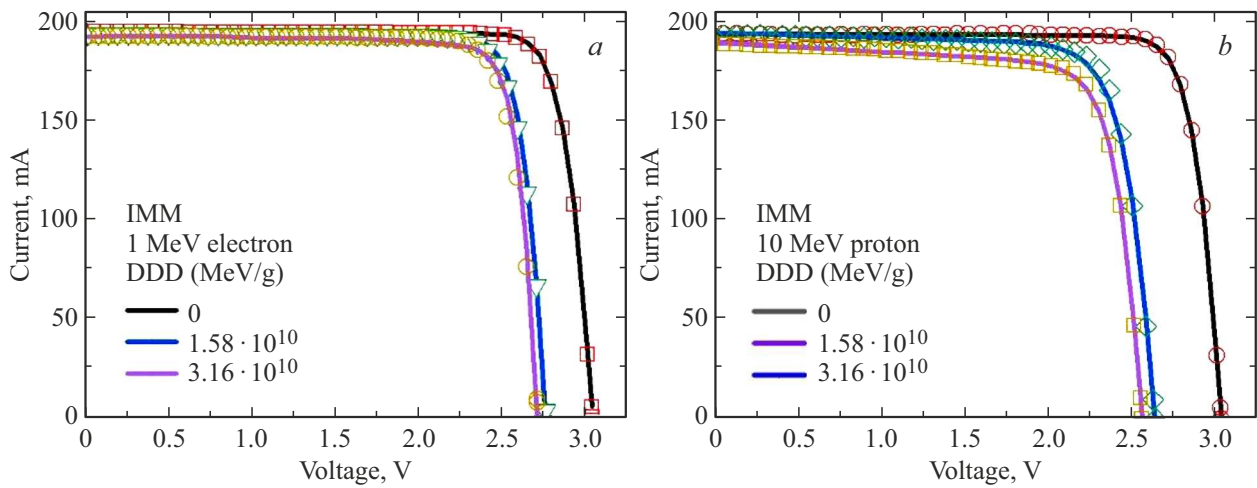


**Figure 2.** Measured and simulated  $I-V$  curves of IMM GaInP/GaAs/InGaAs solar cells irradiated by (a) electron and (b) proton with different DDD (solid line: measured data; symbols: fitting result).

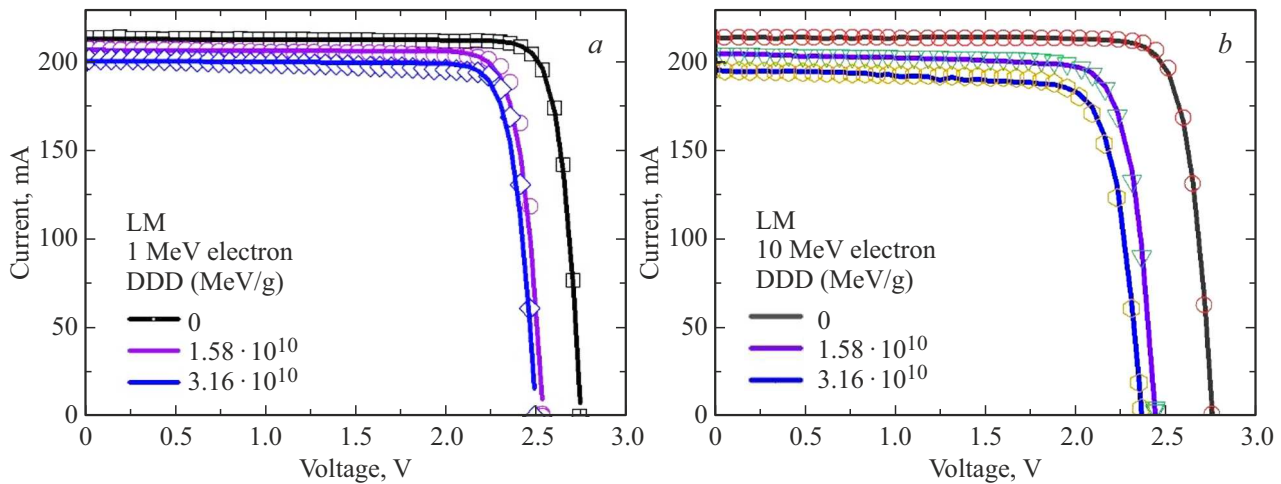


**Figure 3.** Measured and simulated  $I-V$  curves of LM GaInP/InGaAs/Ge solar cells irradiated by (a) electron and (b) proton with different DDD (solid line: measured data; symbols: fitting result).

**Table 2.** Fitted electrical parameters of GaInP/GaAs/InGaAs solar cells irradiated with different DDD

	DDD (MeV/g)	$I_{ph}$ (mA)	$I_0$ (A)	$n$	$R_s$ ( $\Omega$ )	$R_{sh}$ ( $\Omega$ )
1 MeV electron	0	193.8	$5.70 \cdot 10^{-16}$	1.72	0.40	3448
	$1.58 \cdot 10^{10}$	192.8	$2.95 \cdot 10^{-14}$	1.80	0.45	2989
	$3.16 \cdot 10^{10}$	191.6	$1.55 \cdot 10^{-13}$	1.83	0.50	2497
10 MeV proton	0	193.9	$5.70 \cdot 10^{-16}$	1.72	0.40	3448
	$1.58 \cdot 10^{10}$	196.0	$2.10 \cdot 10^{-14}$	1.80	0.47	1964
	$3.16 \cdot 10^{10}$	189.8	$1.40 \cdot 10^{-10}$	1.87	0.56	216

increase of the irradiation doses in IMM solar cells in both proton and electron irradiation, while the degradation of  $I_{sc}$  (short circuit current) is not obvious. And, degradation of both  $V_{oc}$  and  $I_{sc}$  is greater in proton irradiated solar cells

compared to that of electron irradiated solar cells under the same irradiation dose. The extracted electrical parameters of solar cells from the experimental data are listed in Table 2.

Table 2 shows that  $I_0$  and  $R_s$  of solar cells increase, and  $R_{sh}$  decrease after the irradiation. When the irradiation dose is  $3.16 \cdot 10^{10}$  MeV/g, the dark current of solar cells increased three and six times for electron and proton irradiation, respectively. Furthermore, decrease of  $R_{sh}$  and increase of  $R_s$  of solar cells in proton irradiation comparing to electron irradiation. These changes in solar cell electrical parameters are the main reasons for the more serious degradation of  $V_{oc}$  and  $FF$  in proton irradiated solar cells.

### 3.2. Fitting results of LM triple-junction solar cells

The measured and simulated  $I-V$  curves of electron and proton irradiated LM GaInP/InGaAs/Ge solar cells with different irradiation doses are shown in Figure 3, a and b.

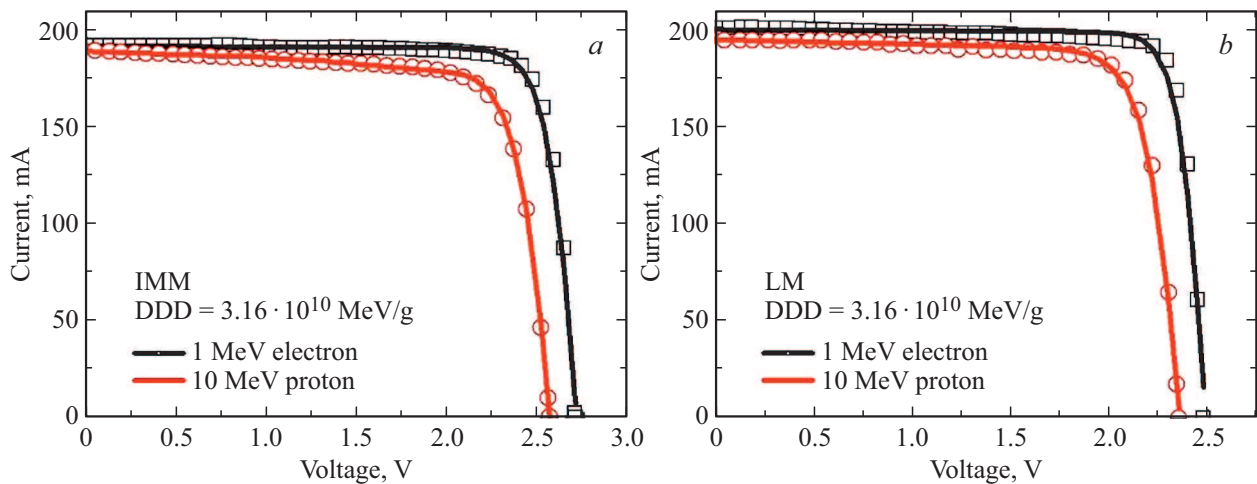


**Figure 4.**  $I$ – $V$  curves of (a) GaInP/GaAs/InGaAs and (b) GaInP/InGaAs/Ge solar cells for  $DDD = 3.16 \cdot 10^{10}$  MeV/g irradiation dose (solid lines: measured curve; symbols: fitting result).

**Table 3.** Fitted electrical parameters of GaInP/InGaAs/Ge solar cells irradiated with different DDD

	DDD (MeV/g)	$I_{ph}$ (mA)	$I_0$ (A)	$n$	$R_s$ ( $\Omega$ )	$R_{sh}$ ( $\Omega$ )
1 MeV electron	0	213	$8.2 \cdot 10^{-17}$	1.62	0.26	3804
	$1.58 \cdot 10^{10}$	206	$8.7 \cdot 10^{-17}$	1.67	0.27	3335
	$3.16 \cdot 10^{10}$	200	$4.5 \cdot 10^{-16}$	1.84	0.33	1591
10 MeV proton	0	214	$1.9 \cdot 10^{-17}$	1.68	0.32	2861
	$1.58 \cdot 10^{10}$	204	$1.8 \cdot 10^{-11}$	1.84	0.41	647
	$3.16 \cdot 10^{10}$	195	$2.7 \cdot 10^{-11}$	1.86	0.46	407

Same as IMM solar cells, the degradation of  $V_{oc}$  is greater than that of  $I_{sc}$ , in both types of irradiation, and the reduction of  $V_{oc}$  and  $I_{sc}$  is greater in proton irradiated solar cells than that of electron-irradiated solar cells. The extracted electrical parameters of solar cells by fitting  $I$ – $V$  curves are listed in Table 3. Same as in IMM solar cells, the  $I_0$  and  $R_s$  of solar cells increase, and  $R_{sh}$  of solar cells decrease after irradiation. The increase of dark current for proton irradiation is also at 6 times of magnitude level.

### 3.3. Comparison of degradation of IMM and LM solar cells

The measured  $I$ – $V$  curves and fitting results of GaInP/GaAs/InGaAs and GaInP/InGaAs/Ge solar cells for electron and proton irradiation with  $DDD = 3.16 \cdot 10^{10}$  MeV/g dose are plotted in Figure 4, a and b, respectively, and changes of extracted parameters are plotted in Figure 5. The results show that proton irradiation caused more degradation in both IMM and LM solar cells, and IMM solar cells showed better radiation resistance than LM solar cells. When the DDD is increased to  $3.16 \cdot 10^{10}$  MeV/g, the  $I_0$  of IMM solar cell under proton irradiation increases by about five

orders of magnitude compared to that of the unirradiated cells. The  $R_{sh}$  decreased to 6.2% of the initial value, and the series resistance  $R_s$  increases by about 1.4 times. In electron irradiated IMM solar cells, the dark current  $I_0$  increased about 271 times,  $R_{sh}$  decreases by 27.6% and  $R_s$  increased about 1.25 times comparing to their initial values in the non-irradiated solar cell. In LM solar cell, when the DDD is increased to  $3.16 \cdot 10^{10}$  MeV/g, dark current  $I_0$  under proton irradiation is increased about six orders of magnitude times and the dark current under electron irradiation increases to about 5 times.

It can be noted in Figure 5 that the increase of  $I_0$  under proton irradiated solar cells is greater and the decrease of  $R_{sh}$  is greater in the electron irradiated solar cells, and the changing trends in electrical parameters under electron and proton irradiation are comparable in both MM and LM solar cells. Degradation of normalized values of  $P_{max}$  in electron and proton irradiated solar cells are shown in Figure 6. From the fitted electrical parameters, it can be concluded that the degradation of both types of solar cells is greater in proton irradiation than that of electron irradiation.

The degradation of solar cell's  $P_{max}$  with increase of irradiation fluence can be predicted by an empirical equation [18], expresses as below

$$\frac{P_\phi}{P_0} = 1 - C \ln \left( 1 + \frac{\phi}{\phi_x} \right), \quad (3)$$

where  $P_0$  is the initial output power,  $P_\phi$  is the solar cell output power after irradiated with  $\phi$  fluence,  $C$  and  $\phi_x$  are the fitting parameters which are related to solar cell structure, types of irradiation particles and its energy. The fitting results of  $\phi_x$  and  $C$  by using Eq. (3) regarding to electron and proton irradiated solar cells, based on the experimental data in Figure 6, are listed in Table 4. The simulation results are quite close to the experimental data but slightly higher, that is because of the triple-junction solar cell structure has not been fully considered in the single

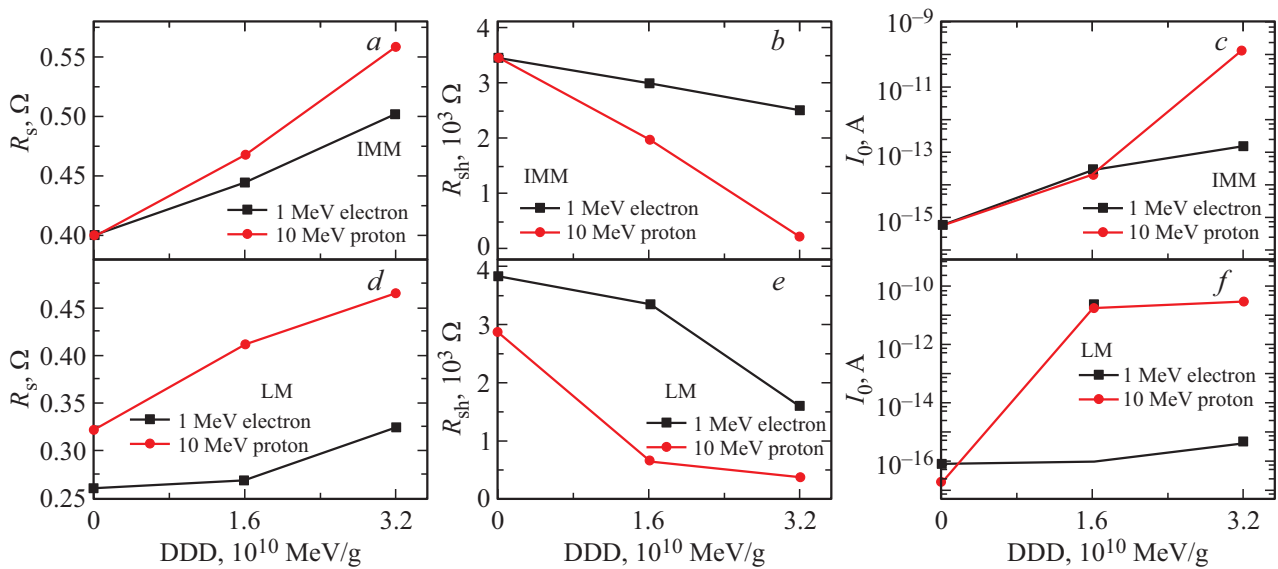


**Figure 5.** Extracted  $R_s$ ,  $R_{sh}$ , and  $I_0$  for GaInP/GaAs/InGaAs (*a, b, c*) and GaInP/InGaAs/Ge (*d, e, f*) solar cells irradiated by electron and proton with different DDD.

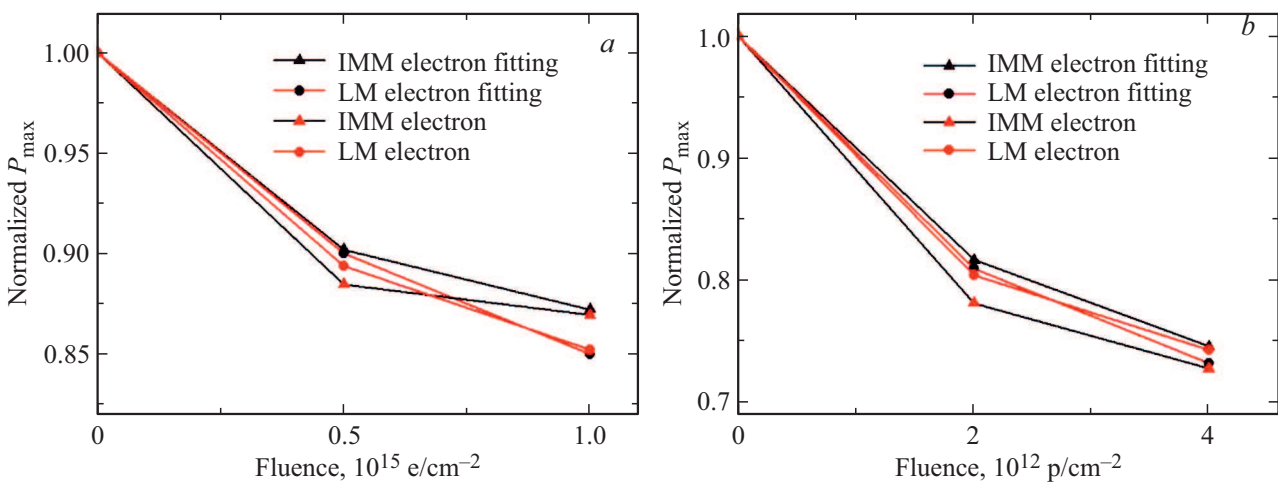


**Figure 6.** Normalized degradation curves of  $P_{max}$  in GaInP/GaAs/InGaAs and GaInP/InGaAs/Ge solar cells with the increase of irradiation fluence, (*a*) electron and (*b*) proton.

**Table 4.** Fitting results for degradation parameters regarding to  $P_{max}$

		C		$\phi_x$	
		Measurement	Fitting	Measurement	Fitting
1 MeV electron	IMM	0.022	0.05	$2.67 \cdot 10^{12}$	$7.27 \cdot 10^{13}$
	LM	0.073	0.10	$1.52 \cdot 10^{14}$	$3.09 \cdot 10^{14}$
10 MeV proton	IMM	0.082	0.12	$1.61 \cdot 10^{11}$	$6.45 \cdot 10^{11}$
	LM	0.099	0.14	$3.48 \cdot 10^{11}$	$7.58 \cdot 10^{11}$

diode model, further studies of the effects of solar cell structure on the simulation model are necessary to obtain more accurate results. These parameters can be used for

evaluating the solar cell electrical parameters regarding to different fluences irradiation regarding to the same energy electron and proton irradiation.

### 3.4. Degradation mechanism of electrical parameters

High energy particle irradiation induces lattice defects in solar cells, which play non-radiative recombination centers and leading to degradation of solar cell electrical parameters. These displacement damages have significant impacts on photogenerated carrier production and recombination [20,21]. Defects in solar cell base region and emission region directly affects the minority lifetime  $\tau$ . The minority lifetime  $\tau$  is inversely proportional to the irradiation dose DDD, and minority carrier diffusion length ( $L$ )

is written as  $L = \sqrt{D\tau}$ , where  $D$  is the minority diffusion coefficient. And, the relationship between the  $L$  and the irradiation fluence  $\phi$  can be expressed as below [22]:

$$\frac{1}{L^2} = \frac{1}{L_0^2} + K_L\phi, \quad (4)$$

where  $L$  and  $L_0$  are the minority carrier diffusion length with and without irradiation by  $\phi$  fluence, and  $K_L$  is the diffusion length damage coefficient. Eq. (4) shows that the minority carrier diffusion length  $L$  decreases with the increase of radiation fluence  $\phi$ , and as a result, the photogenerated minority carriers recombine before reaching the pn junction, and cause the degradation of  $I_{sc}$  and  $I_{ph}$ . The reduction of  $V_{oc}$  and  $I_0$  is related to defects in solar cells [23], and can be expressed as [24]:

$$V_{oc} = \frac{k_B T}{q} \ln\left(\frac{I_{ph}}{I_0} + 1\right), \quad (5)$$

$$I_0 \propto J_s = \frac{qD_n n_{p0}}{L_n} + \frac{qD_p p_{n0}}{L_p}, \quad (6)$$

where  $J_s$  is the reverse saturation current density,  $L_n$  and  $L_p$  are the minority carrier diffusion lengths in the  $p$ -type base region and the  $n$ -type emission region, respectively. After irradiation, the defect density increases and  $L$  decreases, resulting in the increase of  $I_0$ . As can be seen from Eq. (5), the decrease of  $I_{ph}$  and the increase of  $I_0$  leads to the decrease of  $V_{oc}$  continuously when the irradiation dose increases.

The increase of  $R_s$  with the increase of irradiation dose increases, because to the carrier removal effect brought on by defects generated by high-energy particles in solar cells [25], which resulting in reduce of the photogenerated current and increase in  $R_s$ . The decrease of  $R_{sh}$  with the increase of irradiation dose is due to the increase of recombination probability caused by the lattice defects and increase of leakage current. Therefore,  $I_{sc}$  decrease with an increase in  $R_s$  and  $V_{oc}$  decrease with a decrease in  $R_{sh}$  [26], and, the filling factor  $FF$  decreases with the increase in  $R_s$  and the decrease in  $R_{sh}$  [27], as a consequent, the output power of solar cell will decrease.

## 4. Conclusion

The electrical parameters of electron and proton irradiated  $I-V$  curves of IMM GaInP/GaAs/InGaAs and LM GaInP/GaAs/Ge triple-junction solar cells are studied and numerically fitted. Degradation of solar cell performance after irradiation is studied from the perspective of electrical parameters. The electrical parameter degradation trend of the GaInP/GaAs/InGaAs solar cells under 10 MeV proton irradiation is higher than that of 1 MeV electron irradiated solar cells. Both dark current  $I_0$  and parallel resistance  $R_{sh}$  significantly decreased after irradiation, and same degradation trends are also observed in GaInP/GaAs/Ge solar cells. Comparing the two types of irradiation,

the proton irradiation resulted more serious degradation of both GaInP/GaAs/InGaAs and GaInP/GaAs/Ge solar cell electrical parameters. When the irradiation fluence is reached  $3.16 \cdot 10^{10}$  MeV/g, the degradation of dark current  $I_0$  of GaInP/GaAs/Ge solar cells is greater under proton irradiation than that of GaInP/GaAs/InGaAs solar cells. Degradation of maximum output power of solar cells has been simulated by an empirical equation and fitting parameters have been calculated.

## CRedit authorship contribution statement

**Z.X. Wang:** Writing — Original draft, Validation, Software, Methodology, Investigation, Data curation, Conceptualization. **M.Q. Liu:** Writing — original draft, Software, Methodology, Investigation, Formal analysis, Data curation. **T.B. Wang:** Writing — original draft, Validation, Methodology, Investigation. **A. Aierken:** Writing — review & editing, Writing — original draft, Validation, Supervision. Methodology, Funding acquisition, Data curation, Conceptualization. **L. Zhong:** Writing — review & editing, Writing — original draft, Validation, Supervision. Methodology, Data curation, Conceptualization. **M. Li:** Validation, Methodology, Investigation, Conceptualization. **G.H. Tang:** Validation, Methodology, Investigation, Conceptualization.

## Declaration of competing interest

The authors declare that they have no known competing financial interests or personal relationships that could have appeared to influence the work reported in this paper.

## Acknowledgement

This work was supported by Basic research foundation of Yunnan Province (Grant No. 202201AS070019).

## References

- [1] R. Verduci, V. Romano, G. Brunetti, N. Yaghoobi Nia, A. Di Carlo, G. D'Angelo, C. Ciminelli. *Adv. Energy Mater.*, **12**, 2200125 (2022).
- [2] J. Xu, K. Yang, Q. Xu, X. Zhu, X. Wang, M. Lu. *Crystals*, **12**, 670 (2022).
- [3] C. Zhang, J. Zhang, Y. Hao, Z. Lin, C. Zhu. *J. Appl. Phys.*, **110**, 064504 (2011).
- [4] F. Ayala-Mat6, D. Seuret-Jim6nez, J.J. Escobedo-Alatorre, O. Vigil-Gal6n, M. Courel. *J. Renewable and Sustainable Energy*, **9**, 063504 (2017).
- [5] T. Easwarakhanthan, J. Bottin, I. Bouhouch, C. Boutrit. *Int. J. Solar Energy*, **4**, 1 (1986).
- [6] S. Raj, A. Kumar Sinha, A.K. Panchal. *J. Renewable and Sustainable Energy*, **5**, 033105 (2013).
- [7] L.H.I. Lim, Z. Ye, J. Ye, D. Yang, H. Du. *Renewable Energy*, **76**, 135 (2015).
- [8] K. Bouzidi, M. Chegaar, M. Aillerie. *Energy Procedia*, **18**, 1601 (2012).
- [9] M. Haouari-Merbah, M. Belhamel, I. Tob6as, J. M. Ruiz. *Solar Energy Mater. and Solar Cells*, **87**, 225 (2005).

- [10] A.J. Bühler, F. Perin Gasparin, A. Krenzinger. *Renewable Energy*, **68**, 602 (2014).
- [11] A. Sabadus, V. Mihailetschi, M. Paulescu. In (Timisoara, Romania, 2017) p. 040005.
- [12] M.R. AlRashidi, K.M. El-Naggar, M.F. AlHajri. *Int. J. Electrical and Computer Eng.*, **7**(2), 118 (2013).
- [13] G. Kumar, A.K. Panchal. *J. Appl. Phys.*, **114**, 084904 (2013).
- [14] M. Diantoro, T. Suprayogi, A. Hidayat, A. Taufiq, A. Fuad, R. Suryana. *Int. J. Photoenergy*, **2018**, 1 (2018).
- [15] A.A. El Tayyan. *Turk. J. Phys.*, **39**, 1 (2015).
- [16] A.B. Or, J. Appelbaum. *J. Lightwave technol.*, 11 (2012).
- [17] X.B. Shen, A. Aierken, M. Heini, J. H. Mo, Q.Q. Lei, X.F. Zhao, M. Sailai, Y. Xu, M. Tan, Y.Y. Wu, S.L. Lu, Y.D. Li, Q. Guo. *AIP Advances*, **9**, 075205 (2019).
- [18] J. Li, A. Aierken, Y. Zhuang, P.Q. Xu, H.Q. Wu, Q.Y. Zhang, X.B. Wang, J.H. Mo, X. Yang, Q.Y. Chen, S.Y. Zhang, C.R. Yan, Y. Song. *Solar Energy Mater. and Solar Cells*, **224**, 111022 (2021).
- [19] A.M. Humada, M. Hojabri, S. Mekhilef, H.M. Hamada. *Renewable and Sustainable Energy Rev.*, **56**, 494 (2016).
- [20] J.R. Srouf, C.J. Marshall, P.W. Marshall. *IEEE Trans. Nucl. Sci.*, **50**, 653 (2003).
- [21] M. Yamaguchi, C. Amano. *J. Appl. Phys.*, **54**, 5021 (1983).
- [22] J.M. Raya-Armenta, N. Bazmohammadi, J.C. Vasquez, J.M. Guerrero. *Solar Energy Mater. and Solar Cells*, **233**, 111379 (2021).
- [23] N. Dharmarasu, A. Khan, M. Yamaguchi, T. Takamoto, T. Ohshima, H. Itoh, M. Imaizumi, S. Matsuda. *J. Appl. Phys.*, **91**, 3306 (2002).
- [24] J. Li, A. Aierken, Y. Liu, Y. Zhuang, X. Yang, J.H. Mo, R.K. Fan, Q.Y. Chen, S.Y. Zhang, Y.M. Huang, Q. Zhang. *Front. Phys.*, **8**, 631925 (2021).
- [25] S.J. Taylor, M. Yamaguchi, T. Yamaguchi, S. Watanabe, K. Ando, S. Matsuda, T. Hisamatsu, S.I. Kim. *J. Appl. Phys.*, **83**, 4620 (1998).
- [26] G. Hongliang, S. Linfeng, W. Yiyong, S. Qiang, Y. Hui, X. Jingdong, G. Bin. *Nucl. Instrum. Meth. Phys. Res. Section B: Beam Interactions with Mater. and Atoms*, **431**, 1 (2018).
- [27] T.J. McMahon, T.S. Basso, S.R. Rummel. In: *Conference Record of the Twenty Fifth IEEE Photovoltaic Specialists Conference — 1996* (IEEE, Washington, DC, USA, 1996) p. 1291.